Modified effective range analysis of electron scattering from krypton

2014 Phys. Scr. 89 105401

(http://iopscience.iop.org/1402-4896/89/10/105401)

IOP Publishing | Royal Swedish Academy of Sciences Physica Scripta

Phys. Scr. 89 (2014) 105401 (10pp) doi:10.1088/0031-8949/89/10/105401

Modified effective range analysis of electron scattering from krypton

Kamil Fedus

Institute of Physics, Faculty of Physics, Astronomy and Informatics, Nicolaus Copernicus University, Grudziadzka 5, 87-100 Torun, Poland

E-mail: kamil@fizyka.umk.pl

Received 4 October 2013, revised 7 August 2014
Accepted for publication 13 August 2014
Published 17 September 2014

Abstract

The elastic cross sections for electron scattering on krypton from zero energy up to 10 eV have been analyzed by the modified effective range method. A simple model based on the analytical solution of the Schrödinger equation with the polarization potential using explicitly determined scattering phase shifts for the three lowest partial waves describes the elastic differential, integral and momentum transfer cross sections up to the energy threshold of the first inelastic process well. In detail, the contribution of the long-range polarization potential to the scattering phase shift is exactly expressed, while the contribution of the short-range effects is modelled by simple quadratic expressions (the effective range expansions). The effective range parameters are determined empirically by comparison with the latest experimental differential cross sections. Presently, the calculated integral and momentum transfer cross sections are validated against numerous electron scattering experiments and the most recent quantum-mechanical theories. To complete the picture, the two-term Boltzmann analysis is employed to determine the electron transport coefficients; the agreement with the electron swarm experimental data is found to be very good.

Keywords: electron elastic scattering, modified effective range theory, krypton

(Some figures may appear in colour only in the online journal)

1. Introduction

In recent years, the scattering of low-energy electrons by krypton has become a subject of scientific interest. The motivation for studies is related *inter alia* to the search for self-consistent cross-section datasets that are necessary for modeling low-temperature plasmas [1]. In particular, tokamak edge plasmas will involve chemical species rarely studied by theory or by experiment; therefore, some scaling laws and predictive models for converting electron-scattering processes down to thermal energies are needed [2].

Recent progress in electron sources and novel angular electron selectors have allowed beam measurements down to thermal energies and at scattering angles that were hardly accessible in the past. Recent achievements in studies of low-energy e^--Kr interactions include measurements of the total cross section down to 14 meV of impact energy by Kurokawa *et al* [3, 4] and the experimental determination of differential cross sections (DCS) by Cho *et al* [5], Linert *et al* [6] and Zatsarinny, Bartschat and Allan [7] that cover almost the entire angular range of 0–180°. Particularly, in the latter work, the DCS were measured with a double hemispherical electrostatic energy selector with an energy resolution higher than 15 meV. All of these new experimental results combined with the old measurements (for example, see review [8]) provide data that are a very good test of the new theoretical models.

Krypton is an interesting benchmark for theories and is particularly valuable for estimating the importance of relativistic corrections and the short-range components of polarizability. Recently, Zatsarinny and Bartschat validated in several works [7, 9–12] the fully relativistic Dirac-based *B*-spline *R*-matrix close-coupling calculations of elastic and excitation (near-threshold) cross sections against a large amount of experimental data. In the Kr electron-excitation calculations [9], they used 31 physical states of the target plus a pseudostate accounting for the Rydberg states and the ionization continuum, while for the elastic calculations [7], only the ground and one pseudo state were needed.

Earlier models used either Hartree–Fock [13–15] or Dirac-Fock [16–19] codes for the static part of the interaction potential and for the proposed different approaches in treating the effects of electron-atom short-range interactions such as the correlation and exchange including the density functional theory [15], a dipole and quadrupole polarization with a short-range cut-off parameter [17], repulsive dynamic distortion correction [18, 19] and adiabatic exchange [20]. Such extensive efforts are a consequence of the fact that the short-range effects become increasingly important for low electron impact energies [21] in which the dominant long-range dipole polarization is challenged. The inclusion of these effects for many-electron atoms in the frame of many-body theories is not simple, and it is computationally expensive.

Here, an alternative way to discuss the low-energy electron scattering problem is presented, i.e. the inverse procedure using experimental cross sections to derive the scattering phase shifts. This approach is based on the modified effective range theory (MERT) by O'Malley *et al* [22, 23]. MERT, as originally proposed for scattering on the long-range polarization potential in a very low energy range, develops the partial-wave phase shifts (η_l) into a series of k, the electron momentum. For the s-wave and a few higher partial waves (usually p and d) that probe the region of the short-range interaction, the parameters of the $\eta_l(k)$ series (called the effective-range expansions) have to be determined empirically by comparison with some numerical data. MERT in its original formulation and in some modified versions have been widely used for the analysis of integral and momentum transfer cross sections in noble gases and spherical-like (Σ symmetry) molecules (for examples, see [24–31]). However, the applicability of the theory was limited to the very low energy range in the past. Particularly, as shown in the detailed analysis for all of the noble gases by Buckman and Mitroy [32], the upper-energy limit for the validity of the $\eta_l(k)$ series, as proposed in the original MERT formulation [22] for the electron scattering on krypton, is only 0.4 eV.

More recently, an alternative approach to MERT has been proposed by Idziaszek and Karwasz [33, 34]. It consists of calculating the phase shifts due to the long-range polarization potential from the exact Mathieu's solutions of the Schrödinger equation and to introducing the effective-range expansion exclusively for the short-range part of the interaction. In a recent publication, we showed [35] that this alternative method satisfactorily describes electron and positron scattering from helium, argon, molecular hydrogen and methane almost up to the energy threshold for the first inelastic processes.

In this paper, MERT [33, 34] is used to describe the elastic cross sections for electron–krypton collisions up to the impact energy of 10 eV. In particular, it is shown that this simple non-relativistic model used to describe the scattering of spinless particles needs only six parameters to describe the elastic differential, integral and momentum transfer cross sections up to the energy of the first electronic excitation in krypton. To improve the precision in the phase-shift determinations, the analysis is based on the most recent and accurate experimental cross-section datasets by Zatsarinny, Bartschat and Allan [7], which extend over large angular and energy ranges.

This paper is organized as follows: In section 2, the principles of the modified effective range theory are described briefly in the context of electron-krypton interaction. In section 3, the scattering phase shifts are determined in order to calculate differential cross sections (reported in section 4), integral elastic cross sections (in section 5) and momentum transfer cross sections (in section 6). To validate the present approach, momentum transfer data are inserted into the Boltzmann transport equation in order to calculate the electron swarm parameters and then compare them with the experimental data. The conclusions are presented in section 7.

2. Theoretical model

Details of the analytical approach to MERT have been described in previous papers [33–35]. In this section, we will recall only a brief account in the context of the electron-krypton collisions. The relative motion of the electron and atom is described by the radial Schrödinger equation:

$$\left[\frac{\mathrm{d}^2}{\mathrm{d}r^2} - \frac{l(l+1)}{r^2} + \frac{\left(R^*\right)^2}{r^4} + V_S(r) + k^2\right]\Psi_l(r) = 0 \quad (1)$$

where $R^* = \sqrt{\alpha e^2 \mu/\hbar^2}$; this is a typical length scale related to the r^{-4} interaction with α denoting the dipole polarizability, e the elementary charge, μ the reduced mass of the projectile/target system and $\hbar$ the Planck constant. Here, $V_S(r)$ refers to the short-range part of the interaction potential, which includes static and exchange forces that come into play at the small electron-atom distances that are comparable to the size of the atom and in which the atom cannot be treated as a single object. In the MERT approach, $V_S(r)$ is neglected; then, equation (1) is turned into the Mathieu's modified differential equation [22, 23], which possesses the analytical solutions. The short-range effects related to $V_S(r)$ are expressed in terms of some boundary conditions imposed on the wave function at $r \to 0$ and are included explicitly in the framework of MERT. Using the Mathieu function, one can see that the scattering phase shifts experienced by the wave functions of different angular momenta are given by the following relation [22, 23]:

$$\tan\eta_l = \frac{m_l^2 - \tan^2\delta_l + \tilde{B}_l \tan\delta_l\left(m_l^2 - 1\right)}{\tan\delta_l\left(1 - m_l^2\right) + \tilde{B}_l\left(1 - m_l^2\tan^2\delta_l\right)} \quad (2)$$

where $\delta_l = \pi\left(\nu_l - l - 1/2\right)/2$. Here, m_l and ν_l (the Mathieu characteristic exponent) denote the energy-dependent parameters; these parameters have to be determined numerically from the analytical properties of the Mathieu functions (see [33–35]). The contribution of the short-range interaction is manifested in parameter $\tilde{B}_l(k)$, which is related to the additional phase shift that is induced by the short-range potential. This parameter is approximated by the quadratic effective

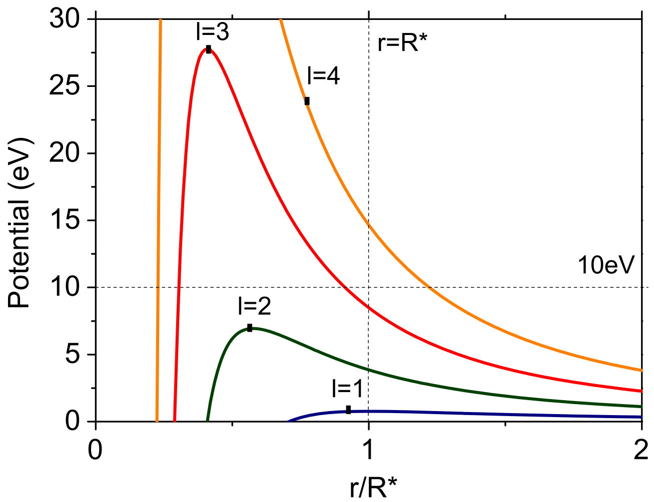

Figure 1. The positive (repulsive) part of the long-range electron–krypton effective potentials for the few lowest partial waves. The distance between the interacting elements is scaled by the characteristic distance R*.

range expansion:

$$\tilde{B}_l(k) \approx B_l(0) + R_l R^* k^2 \big/ 2 + \ldots \quad (3)$$

where R_l can be interpreted as the effective range for a given partial wave. In the particular case of $l = 0$, $B_0(0)$ can be expressed in terms of A, and the s-wave scattering length can be expressed as: $B_0 = -R^* \big/ A$.

To estimate the number of partial waves necessary to be treated by equation (2), one should compare the energy of the projectile with the value of the repulsive long-range potential for each partial wave at the cut-off distance in which the short-range effects disappear. The long-range effective potential is composed of a centrifugal barrier $l(l+1)r^{-2}$ and a dipole polarization term $\left(R^*\right)^2 r^{-4}$. In figure 1, this potential is drawn for the few lowest partial waves in the case of the electron–krypton interaction. In the calculations, a recent experimental value of the polarizability $\alpha = 16.86 a_0^3$ [36] was used. This is slightly lower than the value of $\alpha = 17.3\ a_0^3$, calculated in [7]. It is also assumed ad hoc that the cut-off distance is equal to the characteristic length for r^{-4} interaction, namely $r = R^* = 4.11 a_0$. Such a size for an atom is an overestimate since R^* is larger than the typical radius of the krypton atom $\left(\approx 3a_0\right)$ calculated from the van der Waals equations of state [37].

Consequently, since only purely elastic scattering is of interest in the present analysis, only electron energies below the first electronic excitation, 9.9152 eV [12] are considered. From figure 1, it is clear that the p-wave ($l = 1$) and d-wave ($l = 2$) of the projectile with a kinetic energy of 10 eV are able to overcome the repulsive long-range effective potential at the cut-off distance $\left(r = R^*\right)$ and are thus able to deeply probe the region of the short-range interaction $\left(r < R^*\right)$. On the other hand, the f-wave ($l = 3$) very weakly probes the space of the krypton atom, and the higher partial waves ($l > 3$) cannot overcome the repulsion of the centrifugal barrier at all. Therefore, in the present analysis, only three first partial waves are treated accurately, namely s, p and d. The small contribution of the higher partial waves is described by taking only the leading order contribution to the phase shift:

$$\tan \eta_l(k) \approx \frac{\pi \alpha k^2}{8(l-1/2)(l+1/2)(l+3/2)}, \quad \text{for } l > 2. \quad (4)$$

Equation (4) is exact at the low-energy limit [22], and it can also be reproduced using a first-order Born approximation. Alternatively, one can also describe the contribution of the higher partial waves ($l > 2$) to equation (4) using the higher-order energy terms in the long-range forces contribution to the phase shifts given by Ali and Fraser (equation 12–14 in [38]).

The integral elastic (σ_{IE}), momentum transfer (σ_{MT}) and differential elastic ($\mathrm{d}\sigma/\mathrm{d}\omega$) cross sections are calculated using the standard partial wave expansions:

$$\sigma_{\mathrm{IE}} = \frac{4\pi}{k^2} \sum_{l=0}^{\infty} (2l+1) \sin^2 \eta_l(k) \quad (5)$$

$$\sigma_{\mathrm{MT}} = \frac{4\pi}{k^2} \sum_{l=0}^{\infty} (l+1) \sin^2\left[\eta_l(k) - \eta_{l+1}(k)\right], \quad (6)$$

$$\frac{\mathrm{d}\sigma}{\mathrm{d}\omega} = \frac{1}{k^2} \left| \sum_{l=0}^{\infty} (2l+1) \exp\left(i\eta_l\right) \sin(\eta_l) \mathrm{P}_l(\cos\theta) \right|^2 \quad (7)$$

where θ is the scattering angle. By substituting equations (2) and (3) for the three first partial waves and equation (4) for the higher angular momentum (100 waves in the present analysis) into equations (5)–(7), one gets relations that can be fitted to experimental cross sections in order to determine the unknown (six) parameters of the effective range expansions, namely $\left(A = -R^* \big/ B_0\right)$: the s-wave scattering length, B_1 and B_2: the zero energy contribution of the p- and d-wave, respectively, and R_0, R_1, and R_2: the effective ranges of all three considered waves. All of these parameters approximate the contribution of the short-range part of the interaction potential to the scattering phase shift.

3. Phase shift analysis

Using a typical MERT analysis, which was the type of analysis used in our previous works [33–35], we derived the scattering phase shifts by fitting the model to the experimental total cross sections below the inelastic threshold since they are measured absolutely and extend frequently well below 1 eV of impact energy. However, much more information is included in the elastic DCS. In particular, DCS reflect the dynamics of cross-section variations versus the impact energy (E) and scattering angle (θ). Therefore, in this work, the scattering phase shifts are determined by applying MERT to the most recent DCS measured with the magnetic-field angle analyser, as reported by Zatsarinny *et al* [7]. This experimental technique allows us to extend the range of DCS

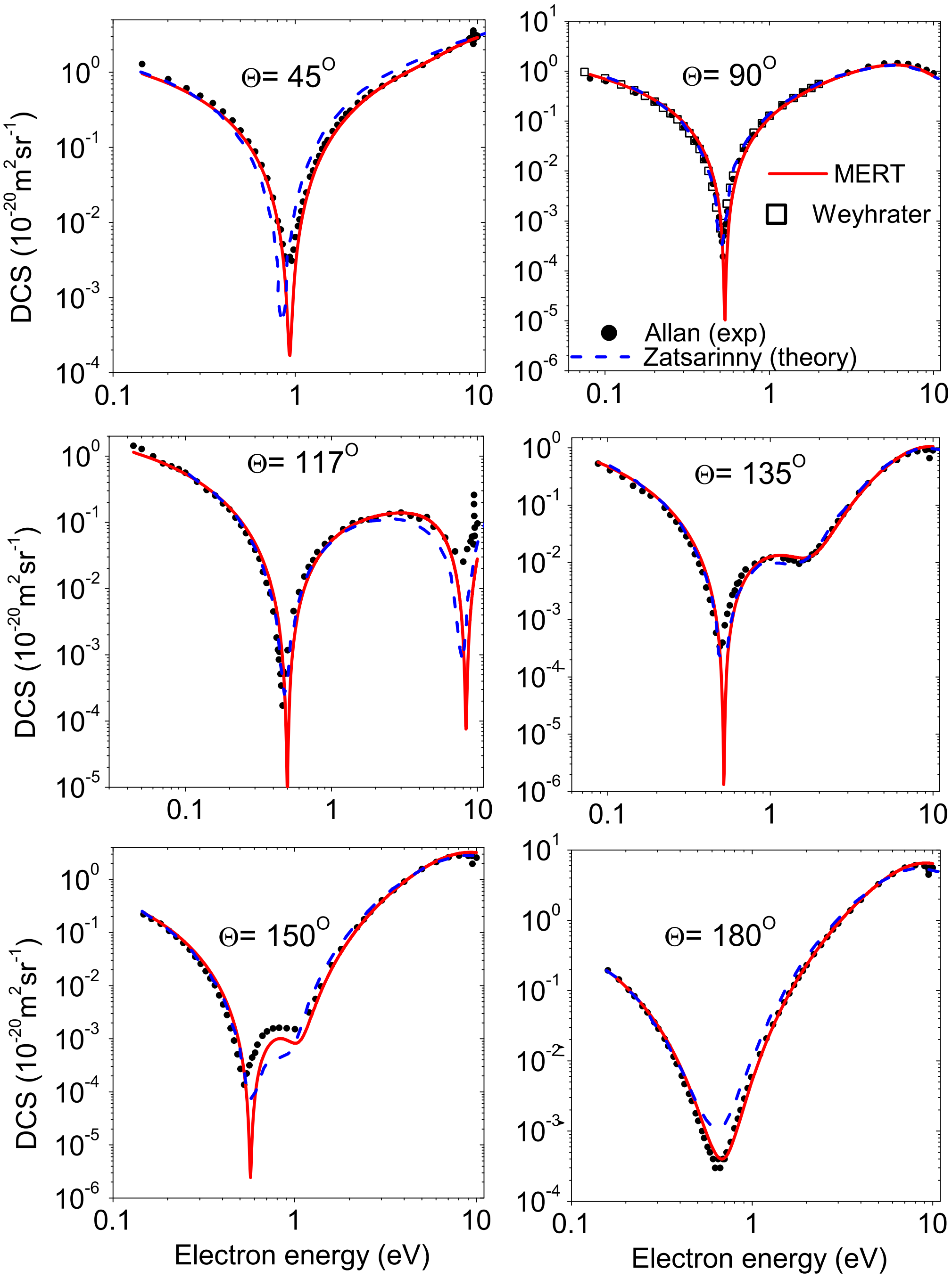

Figure 2. MERT simultaneous fit (solid line) to six elastic differential cross-section datasets measured by Zatsarinny, Bartschat and Allan [7] (dots) at 45°, 90°, 117°, 135°, 150° and 180°. For clarity, not all of the experimental points are presented. The experimental data of Weyhrater *et al* [39] (open squares) for 90° and the B-spline R-matrix calculations (dashed line) of Zatsarinny *et al* [7] are also shown for comparison.

measurements from 0° to 180°, removing ambiguities in the extrapolating data into angles inaccessible in earlier experiments, which thus yields a demanding check for theories. Moreover, the data of Zatsarinny *et al* [7] were obtained in a very wide energy range with very high resolution (15 meV).

Figure 2 presents the results of the simultaneous unweighted least-square fits of equation (7) to six DCS datasets [7] measured at 45°, 90°, 117°, 135°, 150° and 180° from 0.05 to 10.0 eV. For comparison, the very low energy experimental data of Weyhreter *et al* [39] measured at 90° are also shown.

Our MERT fit is in good agreement with not only the experiment but also with the recent relativistic *R*-matrix calculations of Zatsarinny *et al* [7] (dashed line). Moreover, both models give much deeper local minima of the DCS than the experiment, which could be related to the finite angular resolution and the strong dependence of the cross section on the scattering angle, as explained by Zatsarinny *et al* [7].

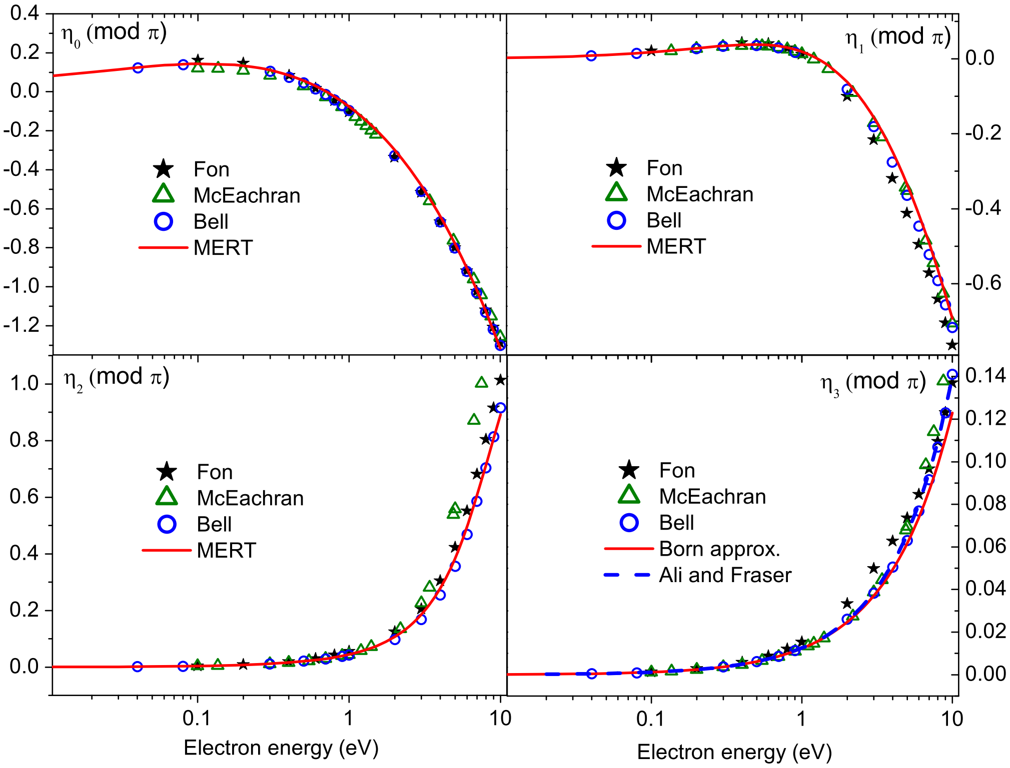

Figure 3. The comparison of the *s*-, *p*- and *d*-wave scattering phase shifts (η_0, η_1 and η_2) derived in the present MERT analysis with the calculations of Fon *et al* [13] (stars), McEachran *et al* [20] (triangles) and Bell *et al* [14] (circles). The *f*-wave phase shift (η_3) calculated in the Born approximation (solid line) using equation (4) and the Ali and Fraser expressions (dashed line) from [38] are also shown.

The derived six parameters of the effective range expansion are given in table 1. In particular, the *s*-wave scattering length $A = -3.486a_0$ is in excellent agreement with the previous experimental and theoretical determinations. The Fano method (i.e. the perturbation of the optical absorption lines) gives values in the range of $-3.03a_0$ to $-3.26a_0$ (see [40] and the references therein). An analysis of the swarm coefficients [41] provides a value of $-3.35a_0$, while the modified effective range analysis (original approach) of the very-low energy DCS by Weyhreter *et al* [39] gives $-3.48a_0$. As expected, the latter result is the same as the value obtained here using the analytical approach to MERT.

The parameters from table 1 were used in equation (2) to calculate the scattering phase shifts, and the results are compared with some other theories in figure 3. The comparative models include the *ab initio* calculations of Fon *et al* [13], McEachran and Stauffer [20] and Bell *et al* [14], which do not similarly take into account the electron spin polarization effects as does the present theory. It is clear from figure 3 that the agreement between the present calculations and the results reported by other authors is very good in the full considered energy range, though the best agreement is obtained with the *R*-matrix theory of Bell *et al* [14].

Figure 3 also compares the *f*-wave phase shift (η_3) calculated in the Born approximation using equation (4) with the chosen reference data. The agreement is very good in the low energy range, but the theory starts to diverge slowly at higher energies when approaching 10 eV. This discrepancy is reduced when the higher-order energy terms of the long-range forces' contribution to the phase shift given by Ali and Fraser (equations 12–14 in [38]) are included. I also checked to ensure that the contribution of the quadrupole polarizability terms present in their expressions is negligable for krypton in the considered energy range. Since the *f*-wave's and the higher partial waves' contributions to the cross sections are small (below 10 eV) when compared to the *s*-, *p*- and *d*-waves, the inclusion of the higher-order terms given by Ali and Fraser [38] do not significantly change the fitting parameters given in table 1.

To validate the present approach, the phase shifts shown in figure 3 were used to calculate the elastic differential, integral and momentum transfer cross sections against numerous experimental data. The results are described in subsequent sections.

Table 1. Parameters of the effective range expansion for the electron scattering from krypton: $A = -R^*/B_0$ (the scattering length), B_1 (zero energy contribution for the *p*-wave), B_2 (zero energy contribution for the *d*-wave), R_0 (*s*-wave effective range), R_1 (*p*-wave effective range) and R_2 (*d*-wave effective range).

	A (a_0)	B_1	B_2	R_0 (a_0)	R_1 (a_0)	R_2 (a_0)
e^--Kr	−3.486	−0.599	0.125	0.533	0.039	0.720

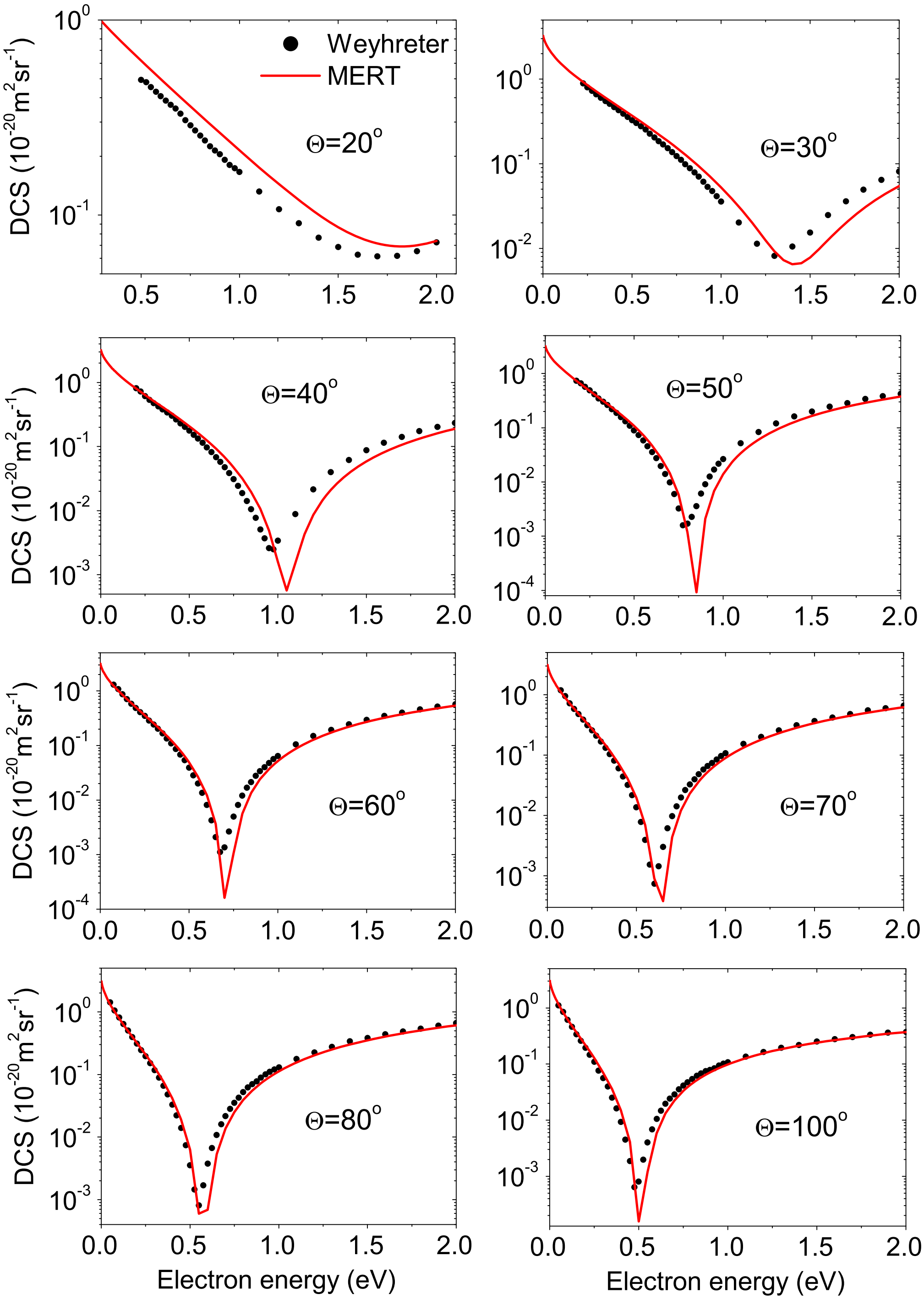

Figure 4. Differential cross section for elastic e$^-$-Kr scattering at angles between 20° and 100° as a function of the projectile energy. The experimental data of Weyhreter *et al* [39] (25 meV energy resolution and 30% absolute DCS value uncertainties) are also compared with the present MERT calculations.

4. Differential cross sections

Figures 4 and 5 show the low-energy (<2 eV) DCS results for the calculated elastic e$^-$-Kr scattering versus the incident electron energy and the scattering angle, respectively. The calculations are compared against the experimental datasets of Zatsarinny, Barstchat and Allan [7] and Weyhreter *et al* [39]. To the best of our knowledge, both sets are the only experimental results available below 2 eV to date. In general, the agreement between the present analysis and the experiments must be judged as good. The present MERT is also consistent with the recent relativistic *R*-matrix calculations [7].

Figure 6 shows the DCS results for elastic e$^-$-Kr scattering at incident electron energies of 5, 7.5 and 10 eV. The present results are in very good agreement with the

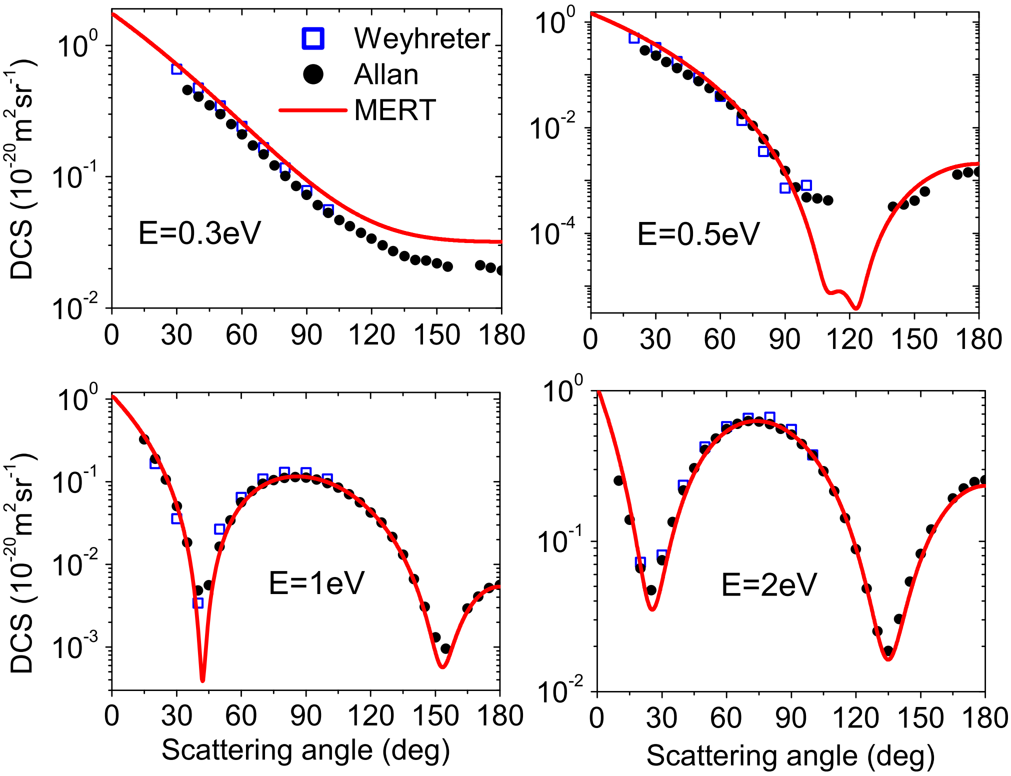

Figure 5. Differential cross section for elastic e$^-$-Kr scattering at electron energies between 0.3 and 2 eV as a function of the scattering angle. The experimental data from Zatsarinny, Barstchat and Allan [7] and Weyhreter *et al* [39] are compared with the present MERT calculations. For clarity, not all of the experimental points are presented.

experimental data of Srivastava *et al* [42] and Danjo [43], which were both obtained with electrostatic energy-analysers and with Cho *et al* [5] (10 eV only) and Linert *et al* [6], which were both obtained with a magnetic angle-changer. An extensive comparison of the different elaborated *ab initio* theories against these experimental sets can be found in [6, 7].

5. Integral elastic cross sections

Our MERT-derived scattering phase shifts (η_l) were introduced into equation (5) to calculate the integral elastic cross sections (σ_{IE}). In the considered energy range ($E < 10$ eV), the elastic cross sections correspond to the total cross sections. The latter were measured in numerous electron beam experiments [44–50]. The comparison between the present results and the experimental total cross sections is shown in figure 7. The present MERT data coincide in the Ramsauer–Townsend minimum with the measurements by the time-of-flight method of Ferch *et al* [48] and by the linear-transmission method with electrostatic optics by Szmytkowski *et al* [50].

Only a few theoretical works [15, 16, 20] describe the integral cross section in the Ramsauer–Townsend minimum; for comparison, the theory of Zatsarinny, Bartschat and Allan [7] is shown in figure 7. Apart from the very low energy limit, the present MERT coincides within 10% with the *R*-matrix relativistic model [7].

Note that the most recent very low-energy experimental data of Kurokawa *et al* [3] are lower than the older results and both of the presented theories at thermal energies. Kitajima *et al* [4] analysed these data using the standard version of MERT. They only obtained a good agreement with the experiment (below 1 eV) when an empirically modified effective range expansion for the *s*-wave phase shift proposed by O'Malley and Crompton [51] was used (see also [35] in which a comparison between different approaches and the original MERT is described).

6. Momentum transfer cross sections

Figure 8 shows the momentum transfer cross sections (σ_{MT} in equation (6)) calculated against the numerous experimental data determined from electron swarm experiments [52–56]. The calculations of Zatsarinny *et al* [7] are also presented for comparison. Though the agreement is good, a stringent test for the presented theoretical results is the analysis of the electron transport coefficients using the Boltzmann transport equation with derived momentum transfer cross sections as the input data. The transport coefficient, such as drift velocity, reduced mobility (μN) and the transverse $\left(D_T/\mu\right)$ and longitudinal $\left(D_L/\mu\right)$ diffusion coefficients, are measured using the electron swarm experiments, which are much more accurate than a typical electron beam technique [1, 57]. Figure 9 presents a two-term analysis of the Boltzmann equation (using a freely accessible *Bolsig*+ solver [58]) that considers

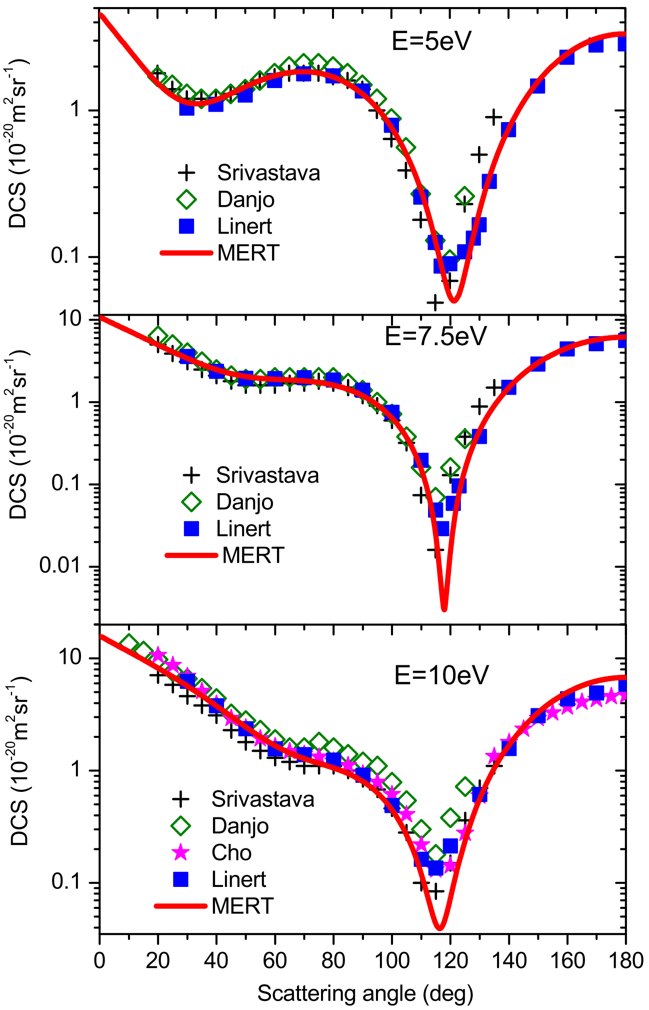

Figure 6. Differential cross section for elastic e$^-$-Kr scattering at electron energies of 5, 7.5 and 10 eV. The experimental data of Srivastava *et al* [42], Danjo [43], Cho *et al* [5] (10 eV only) and Linert *et al* [6] are compared with the MERT results.

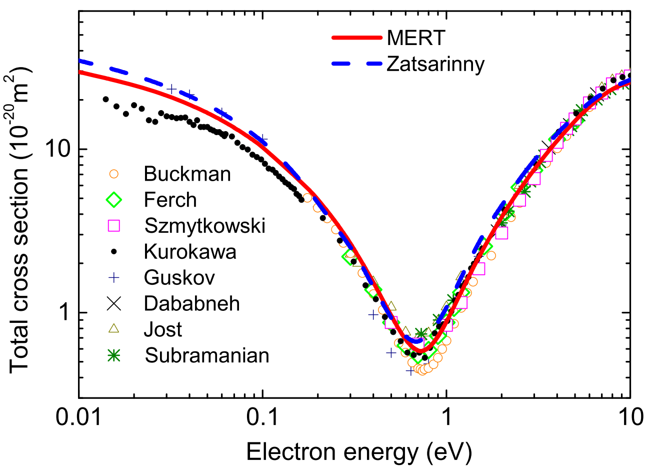

Figure 7. Total cross section for elastic e$^-$-Kr scattering below 10 eV of electron energy. The experimental data of Guskov *et al* [44], Dababneh *et al* [45], Jost *et al* [46], Buckman *et al* [47], Ferch *et al* [48], Subramanian *et al* [49], Szmytkowski *et al* [50] and Kurokawa *et al* [3] are compared with the present calculations and the theory of Zatsarinny *et al* [7].

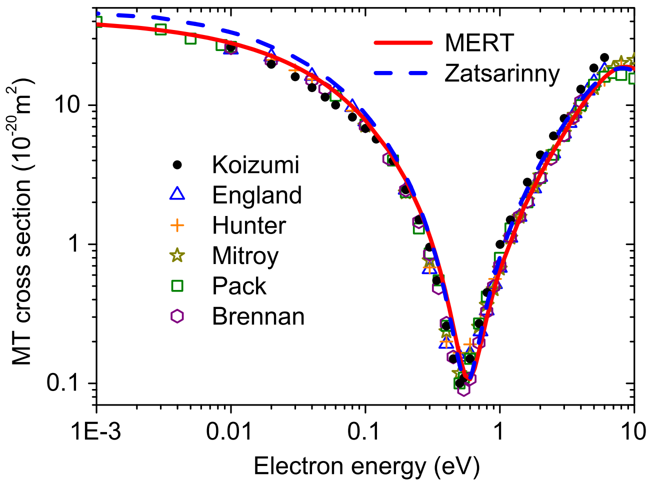

Figure 8. Momentum transfer cross section for elastic e$^-$-Kr scattering below 10 eV of electron energy. The swarm-derived data of Koizumi *et al* [52], England *et al* [53], Hunter *et al* [54], Mitroy [55], Pack *et al* [56] and Brennan *et al* [41] are compared with the present calculations and theory of Zatsarinny *et al* [7].

the present results (solid line) and those by Zatsarinny *et al* [7] (dashed line) as the input data. To include the effects of the first electronic excitation that appears in the proximity of 10 eV, the most recent inelastic cross sections [12] that describe this process were used. The calculations are compared with experimental results [41, 52, 54, 56, 59–61] up to 10 Td of the reduced electric field (E/N). The agreement of the present MERT with the experiments is generally good within the spread of the experimental data in the whole range of reduced fields for all four swarm parameters. Although some (small) discrepancies can be noticed at a very low E/N for the drift velocity and reduced mobility, the same behaviour is nevertheless observed when using momentum transfer cross sections calculated by Zatsarinny, Bartschat and Allan [7]. Very elaborate comparisons of different cross-section datasets for electron–krypton collisions in the context of a swarm coefficients analysis can be found in the recently published work [1]. The present Boltzmann analysis is principally done to show that the effective range parameters are determined in this work (table 1) and to define the momentum transfer elastic cross sections with similar accuracy, as more advanced quantum mechanical calculations have been recently introduced. Hence, the present semi-empirical model can be used to parameterize the cross sections in the entire energy region for elastic scattering.

7. Conclusions

It has been shown that the modified effective theory (MERT) in the form proposed by Idziaszek and Karwasz [33] can be used to describe the elastic differential, integral and momentum transfer cross sections for electron–krypton collisions up to 10 eV, i.e. the threshold for the first inelastic process. This proves that electron scattering from Kr is

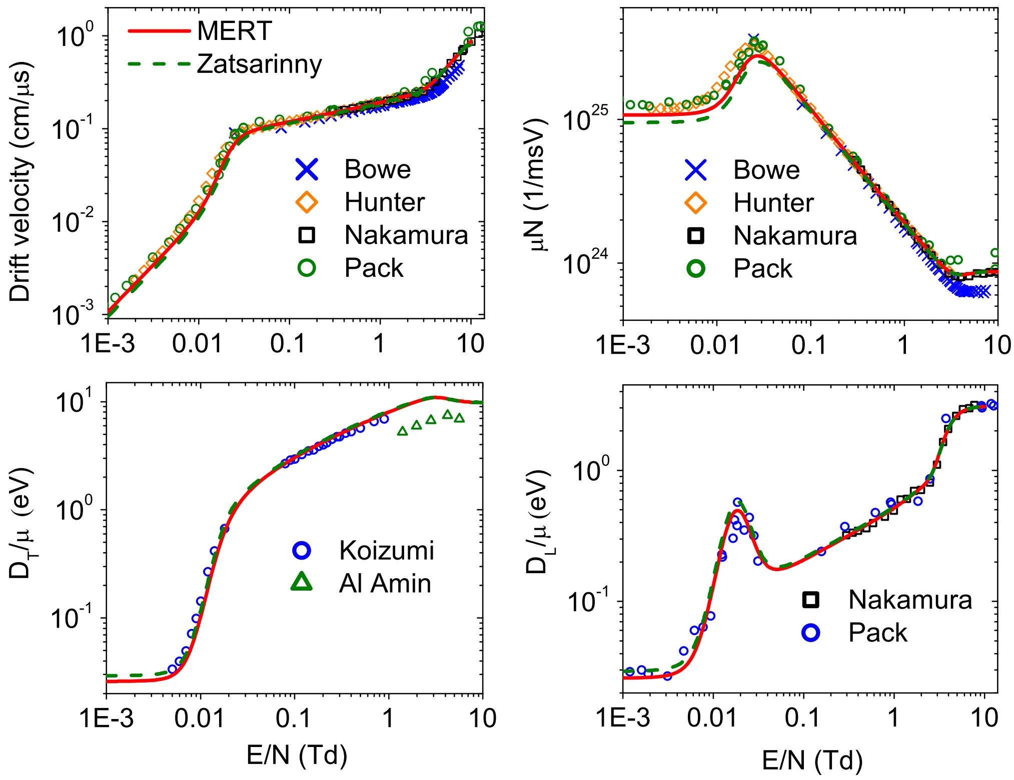

Figure 9. Swarm parameters: drift velocity, mobility × gas density (μN), transverse $\left(D_T/\mu\right)$ and longitudinal $\left(D_L/\mu\right)$ diffusion coefficients for elastic e^--Kr scattering below 10 Td of the reduced electric field (E/N). The experimental data of Koizumi *et al* [52], Hunter *et al* [54], Pack *et al* [56], Bowe [59], Nakamura *et al* [60] and Al Amin *et al* [61] are compared with two-term Boltzmann analysis [58] using a momentum transfer cross section calculated in this work (solid line) and predicted by the theory of Zatsarinny *et al* [7] (dashed line).

dominated by the long-range polarization potential in the whole energy range for elastic scattering, while the short-range effects can be simply included within a frame of boundary conditions imposed on the wave function, which is the solution of the Schrödinger equation with pure polarization potential. Also, it shows that the contribution of the short-range interaction to the scattering phase shifts of s, p and d- partial waves can be very well approximated by simple quadratic expressions.

However, we write in the final that a simple semi-empirical (geometrical) model, such as MERT, cannot be treated as a real alternative to the advanced *ab initio* calculations. MERT does not take into account all of the aspects of complex many-body interactions between the incoming electrons and atoms. In particular, it does not include all of the subtle contributions of spin and relativistic effects. Nevertheless, this model has some major advantages such as a very intuitive description of low-energy electron–atom collisions; more practically, it provides a relatively simple relation for the scattering phase shifts that can be utilized for the parameterization of elastic cross sections for different atoms in a wide energy range. In particular, in this work, it has been shown that only six parameters of the effective range expansions are sufficient to define cross sections in a large low energy range for electron–krypton elastic scattering. Furthermore, the present results indicate that the spin–orbit interaction and other relativistic effects in the case of elastic scattering of low-energy electrons from krypton might not be as significant as we were once led to believe. Finally, the present results suggest that using MERT as the approach when it is formulated within the inverse scattering procedure could be very useful for recovering unknown electron-atom potentials from a set of electron scattering data. For this to take place, however, more theoretical efforts are needed; in particular, the physical interpretation of the parameters derived via the effective range expansions must be understood. It would also be useful to relate them to other short-range parameters appearing in some *ab initio* theories [15, 17].

Acknowledgments

The author thanks Prof. M Allan for sending extensive numerical sets of his experimental results, Dr Z Idziaszek for providing detailed explanations of the MERT numerical package and Prof. G Karwasz for introducing the subject of electron collisions. We also acknowledge the financial support of the Foundation for Polish Science within the START frame.

References

[1] Bordage M C, Biagi S F, Alves L L, Bartschat K, Chowdhury S, Pitchford L C, Hagelaar G J M, Morgan W L, Puech V and Zatsarinny O 2013 *J. Phys. D: Appl. Phys.* **46** 334003

[2] Karwasz G and Fedus K 2013 *Fus. Sci. Tech.* **63** 338 http://www.ans.org/pubs/journals/fst/a_16440

[3] Kurokawa M, Kitajima M, Toyoshima K, Kishino T, Odagiri T, Kato H, Hoshino M, Tanaka H and Ito K 2011 *Phys. Rev.* A **84** 062717

[4] Kitajima M, Kurokawa M, Kishino T, Toyoshima K, Odagiri T, Kato H, Anzai K, Hoshino M, Tanaka H and Ito K 2012 *Eur. Phys. J.* D **66** 130

[5] Cho H, Gulley R J and Buckman S J 2003 *J. Korean Phys. Soc.* **42** 71 http://www.kps.or.kr/jkps/abstract_view.asp?articleuid=DB97C584-4D64-46F2-94AE-0125972D660C&globalmenu=3&localmenu=10

[6] Linert I, Mielewska B, King G C and Zubek M 2010 *Phys. Rev.* A **81** 012706

[7] Zatsarinny O, Bartschat K and Allan M 2011 *Phys. Rev.* A **83** 032713

[8] Zecca A, Karwasz G P and Brusa R S 1996 *Rev. Nuovo Cim.* **19** 1–146

[9] Bartschat K and Zatsarinny O 2007 *J. Phys.* B **40** F43

[10] Hoffmann T H, Ruf M-W, Hotop H, Zatsarinny O, Bartschat K and Allan M 2010 *J. Phys.* B **43** 085206

[11] Zatsarinny O and Bartschat K 2010 *J. Phys.* B **43** 074031

[12] Allan M, Zatsarinny O and Bartschat K 2011 *J. Phys.* B **44** 065201

[13] Fon W C, Berrington K A and Hibbert A 1984 *J. Phys.* B **17** 3279

[14] Bell K L, Berrington K A and Hibbert A 1988 *J. Phys.* B **21** 4205

[15] Gianturco F A and Rodriguez-Ruiz J A 1994 *Z. Phys.* D **31** 149

[16] Sin Fai Lam L T 1982 *J. Phys.* B **15** 119

[17] Sienkiewicz J E and Baylis W E 1991 *J. Phys.* B **24** 1739

[18] Mimnagh D J R, McEachran R P and Stauffer A D 1993 *J. Phys.* B **26** 1727

[19] McEachran R P and Stauffer A D 2003 *J. Phys.* B **36** 3977

[20] McEachran R P and Stauffer A D 1984 *J. Phys.* B **17** 2507

[21] Field D, Lunt S L and Ziesel J P 2001 *Acc. Chem. Res.* **34** 291

[22] O'Malley T F, Spruch L and Rosenberg L 1961 *J. Math. Phys.* **2** 491

[23] O'Malley T F, Rosenberg L and Spruch L 1962 *Phys. Rev.* **125** 1300

[24] O'Malley T F 1963 *Phys. Rev.* **130** 1020

[25] Chang E S 1981 *J. Phys.* B **14** 893

[26] Ferch J, Granitza B and Raith W 1985 *J. Phys.* B **18** L445

[27] Buckman S J and Lohmann B 1986 *J. Phys.* B **19** 2547

[28] Schmidt B 1991 *J. Phys.* B **24** 4809

[29] Isaacs W A and Morrison M A 1992 *J. Phys.* B **25** 703

[30] Mann A and Linder F 1992 *J. Phys.* B **25** 533

[31] Lunt S L, Randell J, Ziesel J P, Mrotzek G and Field D 1998 *J. Phys.* B **31** 4225

[32] Buckman S J and Mitroy J 1989 *J. Phys.* B **22** 1365

[33] Idziaszek Z and Karwasz G 2006 *Phys. Rev.* A **73** 064701

[34] Idziaszek Z and Karwasz G 2009 *Eur. Phys. J.* D **51** 347

[35] Fedus K, Karwasz G P and Idziaszek Z 2013 *Phys. Rev.* A **88** 012704

[36] Olney T N, Cann N M, Cooper G and Brion C E 1997 *Chem. Phys.* **223** 59

[37] Szmytkowski R 1995 *Phys. Rev.* A **51** 853

[38] Ali M K and Fraser P A 1977 *J. Phys.* B **10** 3091

[39] Weyhreter M, Barzik B, Mann A and Linder F 1988 *Z. Phys.* D **7** 333

[40] Rupnik K, Asaf U and Mcglynn S P 1990 *J. Chem. Phys.* **92** 2303

[41] Brennan M J and Ness K F 1993 *Austr. J. Phys.* **46** 249

[42] Srivastava S K, Tanaka H, Chutjian A and Trajmar S 1981 *Phys. Rev.* A **23** 2156

[43] Danjo A 1988 *J. Phys.* B **21** 3759

[44] Gus'kov Y K, Savvov R V and Slobodyanyuk V A 1978 *Sov. Phys.-Tech. Phys.* **23** 167

[45] Dababneh M S, Kauppila W E, Downing J P, Laperriere F, Pol V, Smart J H and Stein T S 1980 *Phys. Rev.* A **22** 1872

Dababneh M S, Hsieh Y F, Kauppila W E, Pol V and Stein T S 1982 *Phys. Rev.* A **26** 1252

[46] Jost K, Bisling P G F, Eschen F, Felsmann M and Walther L 1983 *Abstracts of Contributed Papers, 13th International Conference on the Physics of Electronic and Atomic Collisions* ed J Eichler, W Fritsch, I V Hertel, N Stolterfoht and U Wille (Amsterdam: North-Holland) p 91

[47] Buckman S J and Lohmann B 1987 *J. Phys.* B **20** 5807

[48] Ferch J, Simon F and Strakeljahn G 1987 *Abstracts of Contributed Papers, 15th International Conference on the Physics of Electronic and Atomic Collisions* ed J Geddes, H B Gilbody, A E Kingston, C J Latimer and H J R Walters (Amsterdam: North-Holland) p 132

[49] Subramanian K P and Kumar V 1987 *J. Phys.* B **20** 5505

[50] Szmytkowski C, Maciąg K and Karwasz G 1996 *Phys. Scr.* **54** 271

[51] O'Malley T F and Crompton R W 1980 *J. Phys.* B **13** 3451

[52] Koizumi T, Shirakawa E and Ogawa I 1986 *J. Phys.* B **19** 2331

[53] England J P and Elford M T 1988 *Aust. J. Phys.* **41** 701

[54] Hunter S R, Carter J G and Christophorou L G 1988 *Phys. Rev.* A **38** 5539

[55] Mitroy J 1990 *Aust. J. Phys.* **43** 19 http://www.publish.csiro.au/paper/PH900019.htm

[56] Pack J L, Voshall R E, Phelps A V and Kline L E 1992 *J. Appl. Phys.* **71** 5363

[57] Cho H, Yoon J S and Song M Y 2013 *Fus. Sci. Tech.* **63** 349 http://www.ans.org/pubs/journals/fst/a_16441

[58] Hagelaar G J M and Pitchford L C 2005 *Plasma Sources Sci. Techn.* **14** 722

[59] Bowe J C 1960 *Phys. Rev.* **117** 1411

[60] Nakamura Y 1990 Electron swarm parameters in krypton and its momentum transfer cross sections *Nonequilibrium Effects in Ion and Electron Transport* ed J W Gallagher, D F Hudson, E E Kunhardt and R J Van Brunt (NY: Plenum Press)

[61] Al-Amin S A and Lucas J 1987 *J. Phys.* D **20** 1590